

# Rotation and oblique pulsation in *Kepler* observations of the roAp star KIC 10483436

L. A. Balona,<sup>1\*</sup> M. S. Cunha,<sup>2</sup> M. Gruberbauer,<sup>3</sup> D. W. Kurtz,<sup>4</sup> H. Saio,<sup>5</sup> T. R. White,<sup>6</sup> J. Christensen-Dalsgaard,<sup>7</sup> H. Kjeldsen,<sup>7</sup> J. L. Christiansen,<sup>8</sup> J. R. Hall<sup>9</sup> and S. E. Seader<sup>8</sup>

<sup>1</sup>South African Astronomical Observatory, PO Box 9, Observatory 7935, Cape Town, South Africa

<sup>2</sup>Centro de Astrofísica e Faculdade de Ciências, Universidade do Porto, 4150-Porto, Portugal

<sup>3</sup>Department of Astronomy & Physics, Saint Mary's University, Halifax, NS B3H 3C3, Canada

<sup>4</sup>Jeremiah Horrocks Institute of Astrophysics, University of Central Lancashire, Preston PR1 2HE

<sup>5</sup>Astronomical Institute, Graduate School of Science, Tohoku University, Sendai 980–8578, Japan

<sup>6</sup>Sydney Institute for Astronomy (SIfA), School of Physics, University of Sydney, NSW 2006, Australia

<sup>7</sup>Department of Physics and Astronomy, Building 1520, Aarhus University, 8000 Aarhus C, Denmark

<sup>8</sup>SETI Institute/NASA Ames Research Center, Moffett Field, CA 94035, USA

<sup>9</sup>Orbital Sciences Corporation/NASA Ames Research Center, Moffett Field, CA 94035, USA

Accepted 2011 January 11. Received 2011 January 7; in original form 2010 December 18

## ABSTRACT

Photometry of KIC 10483436 was obtained continuously with 1-min exposures over a 27-d period from the *Kepler* satellite. The light curve shows rotational variations from surface spots with a period of  $4.303 \pm 0.002$  d, an amplitude of about 6 mmag and eight pulsation frequencies typical of roAp stars. The high-frequency pattern consists of a quintuplet of equally spaced peaks where the frequency of the dominant central peak (68  $\mu$ mag amplitude) is 1353.00  $\mu$ Hz ( $P = 12.32$  min). A second set of three peaks of lower amplitude are also visible. These appear to form part of a quintuplet centred on 1511.6  $\mu$ Hz with the central peak and one side peak missing. The equidistant frequency spacing is 2.69  $\mu$ Hz, which corresponds to the 4.303 d rotation period. However, the amplitudes (12  $\mu$ mag) of these peaks are too close to the detection level to allow definite identification of the multiplets. Although no spectrum is available, the character of the pulsations shows that this is a roAp star with two high-frequency modes modulated in amplitude in accordance with the oblique pulsator model. The 4.303-d variation in the light curve, which is interpreted as rotational modulation, shows harmonics as high as the 26th. These harmonics are probably a result of many patches of varying surface brightness associated with surface abundance variations characteristic of Ap stars.

**Key words:** stars: chemically peculiar – stars: individual: KIC 10483436 – stars: oscillations.

## 1 INTRODUCTION

The *Kepler* mission is designed to detect Earth-like planets around solar-type stars by the transit method (Borucki et al. 2010; Jenkins et al. 2010; Koch et al. 2010). *Kepler* is continuously monitoring the brightness of about 150 000 stars for at least 3.5 yr in a 105-deg<sup>2</sup> fixed field of view. In the course of the mission, extremely precise photometry of each star is being obtained. Analysis of results shows that the median noise level in the periodogram for a star of magnitude 10 is about 0.9  $\mu$ mag for an observing run of 30 d. For a star of magnitude 12, the corresponding median noise level is 2.4  $\mu$ mag. These values apply to a frequency range 0–20 d<sup>-1</sup>, the

noise level dropping slowly towards higher frequencies. Rather than the median, it is somewhat more convenient to use the top-of-the-noise peaks as a measure of the noise level in the periodogram. We refer to this as the ‘grass’ level. The grass level is approximately 2.5 times higher than the median noise level.

The coolest subgroup of Ap stars is the SrCrEu group ( $6400 \leq T_{\text{eff}} \leq 10\,000$  K). Kurtz (1982) discovered that while most of these stars do not show any oscillations, some exhibit single or multiperiodic pulsations with periods in the range 4–21 min (the roAp stars). Over 40 roAp stars are known. Ap stars which have been observed in searches for high-frequency pulsations but show no evidence for the latter are named non-oscillating Ap (noAp) stars (North et al. 1997).

In some roAp stars, there are frequency multiplets which have spacings equal to the frequency of rotation of the star. Kurtz (1982)

\*E-mail: lab@sao.ac.za

interpreted these observations in terms of a dipole mode symmetric around the magnetic axis, tilted with respect to the rotational axis (the oblique pulsator model). As the star rotates, the inclination of the pulsation axis changes, leading to changes in the observed pulsational amplitude. In the periodogram, a pure dipole mode is then represented by a triplet structure centred on the oscillation frequency. Considerations about the magnetic field effect on the oscillations introduce changes to this picture. The additional restoring force, of importance in the outer layers of the star, will distort the axisymmetric dipole mode in such a way that it will be described by a sum of spherical harmonics of different degrees,  $l$  (Dziembowski & Goode 1996; Cunha & Gough 2000; Saio & Gautschy 2004). The same modulation effect will apply to each spherical harmonic component of the eigenmode and in general the observer will no longer see a triplet, but, instead, a larger multiplet structure (Saio & Gautschy 2004). In the cases when the effect of rotation on the oscillations is comparable to that of the magnetic field, the situation is modified further. Such a situation was considered by Bigot & Dziembowski (2002) and Gough (2005) under the assumption that the dipole mode can still be described by a single spherical harmonic. The authors found that as a result of the combined effects of the Lorentz force and centrifugal distortion of the star, the pulsation and magnetic axes are no longer aligned. In addition, the effect of the Coriolis force introduces an asymmetry in the amplitudes of the side peaks of the multiplet in the observer's system, as found, for example, in the well-studied roAp star HR3831.

A further consequence of the presence of non-spherically symmetric agents on the oscillations, such as those mentioned above, is the removal (partially, in the case of the Lorentz or centrifugal forces, or totally, in the case of Coriolis forces) of the frequency degeneracy among the  $2l + 1$  modes associated with a given radial order  $n$  and spherical degree  $l$ . However, in roAp stars only one of these modes is observed, for a given  $l$ . This means that some selection effect must be in action, connected either with the excitation or with the damping of modes of the same degree, but different orientation on the stellar surface. Within the interpretation of the oblique pulsator model, the mode that is observed is that which is axisymmetric about the magnetic field axis.

A possible explanation for why that mode is preferentially excited was proposed by Balmforth et al. (2001) who argued that the strong magnetic field present in roAp stars is likely to suppress convection around the magnetic poles. Since the absence of convection is believed to help the excitation of the high-radial-order oscillations observed in roAp stars (Balmforth et al. 2001; Cunha 2002; Saio 2005; Théado et al. 2009), the modes of highest amplitude near the magnetic poles will be preferentially excited. If the magnetic field effect on the oscillations dominates over the rotation effect, then the interpretation suggested by these authors remains possible. However, if rotation cannot be neglected, there will no longer be a mode axisymmetric about the magnetic axis and thus an alternative selection mechanism needs to be considered.

The roAp stars that show multiplets due to rotation all have short rotational periods ( $1.9 < P < 12.5$  d) and relatively high projected rotational velocities ( $13 < v \sin i < 33$  km s<sup>-1</sup>). Most roAp stars do not show these multiplets either because the rotational period is too long (and the multiplets unresolved) or because they have amplitudes below the threshold of detectability. Many do, however, show multiple frequencies which can sometimes be interpreted in terms of magnetically perturbed acoustic modes with the same low degree,  $l$ , and of consecutive high radial orders,  $n$ . When their separation in frequency is approximately constant, measurements

of the frequency spacing (the large separation) allows an estimate of the mean density of the star.

Prior to launch there were no known roAp stars in the *Kepler* field of view, though several stars in the field are classified as Ap. Recently, *Kepler* observations of one such star, KIC 8677585 (BD+44 3063, ILF1+44 20) showed pulsations typical of roAp stars (Balona et al. 2011). While multiple pulsation frequencies were found in that star, no multiplet structures were identified. Furthermore, no light variation which could be attributed to the rotation of the star was found. Such a variation, caused by patches of different surface chemical composition, is common in Ap stars. Its absence in KIC 8677585 photometric data spanning an interval of 9.73 d suggests that the star has a much longer period of rotation. It should be noted that long-term drifts are present in the *Kepler* data, which means that the interpretation of long-term behaviour has to be made with caution.

Analysis of short-cadence data from the quarter-2 *Kepler* release of  $\delta$  Sct candidates revealed that KIC 10483436 (J2000: 19:46:29, +47:37:50,  $V = 11.43$ ) also pulsates with frequencies typical of roAp stars. A query of the SIMBAD reveals no objects within a radius of 1 arcmin of this position. No previous observations of the star have been published. The field around the star is relatively uncrowded. Through the remainder of this paper, we will discuss the *Kepler* data on KIC 10483436.

## 2 PHYSICAL PARAMETERS

The *Kepler* data for KIC 10483436 consists of 39 295 continuous photometric data points taken during the time-interval (truncated) BJD 550 64.362–550 91.477 (27.11 d). These are short-cadence exposures obtained in a 58.85 s cycle, of which the effective exposure time is 54.18 s, as described by Gilliland et al. (2010). The ‘uncorrected’ data used here consist of aperture photometry. The only ground-based photometric observations for KIC 10483436 consist of five-colour photometry using Sloan filters from the Kepler Input Catalogue (KIC). The KIC also contains a number of derived quantities including the stellar radius in units of solar radius,  $R/R_{\odot}$ , the effective temperature,  $T_{\text{eff}}$ , and the surface gravity  $\log g$ . While there is no guarantee that these values are appropriate for the peculiar atmospheres of the Ap stars, the values derived for KIC 10483436 are typical of roAp stars; thus, we accept them for our analysis in this paper. Future spectroscopy will provide more confident measures. They are  $R = 1.605 R_{\odot}$ ,  $T_{\text{eff}} = 7388$  K,  $\log g = 4.152$ , and  $[\text{Fe}/\text{H}] = 0.284$ . From these we derive for the star's luminosity,  $L$ ,  $\log L/L_{\odot} = 0.838$ . Since there is no information available on how the KIC parameters were obtained, we do not have any reliable means of estimating the errors in the effective temperature and luminosity. The typical error in the photometric determinations of the effective temperature for A-type stars is about 200 K. If we assume an error of about 0.5 mag in the absolute magnitude, which again is a typical error obtained from photometric calibrations, we obtain an error of 0.2 in  $\log L/L_{\odot}$ .

Stellar parameters for Ap stars are difficult to obtain because of the line blanketing and chemical inhomogeneity. Normal photometric calibration procedures do not apply to Ap stars and the above parameters are likely to be only a rough estimate. In Fig. 1, we show the location of KIC 10483436 in the theoretical Hertzsprung–Russell (HR) diagram and compare it with other roAp stars and with noAp stars for which temperatures and luminosities are available in the literature. The error bars shown for KIC 10483436 are those discussed above. The first roAp star discovered from the *Kepler* data, KIC 8677585, is also shown in the figure. Like KIC 8677585,

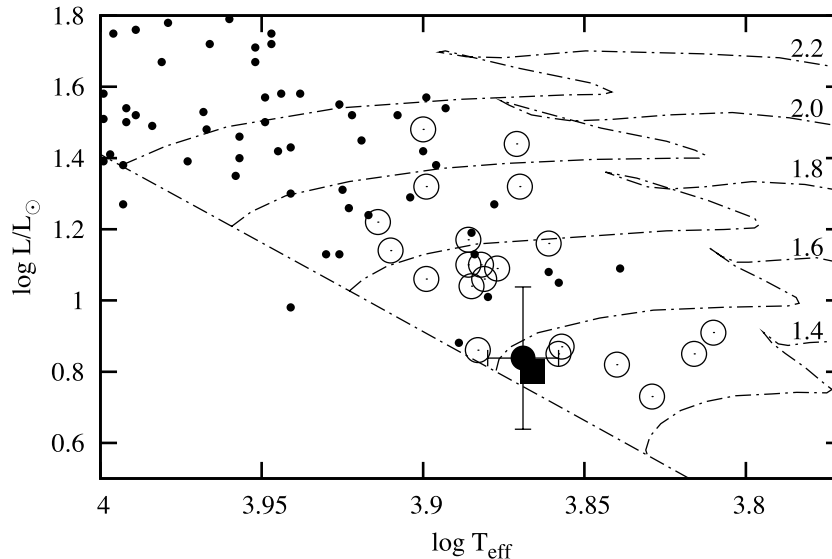


**Figure 1.** Location of the roAp stars (open circles) and noAp stars (small filled circles) in the theoretical HR diagram. Also shown is the zero-age main sequence and several evolutionary tracks labelled in solar masses. The location of KIC 8677585 is shown by the filled square and that of KIC 10483436 by the filled circle and error bars.

KIC 10483436 appears to be close to the zero-age main sequence and with an effective temperature close to the mean value for the roAp stars. However, further observations will be required to confirm the effective temperature and luminosity.

### 3 THE ROTATION PERIOD

The most obvious variability in KIC 10483436 is a periodic variation with a peak-to-peak amplitude of about 12 mmag (Fig. 2). The raw data show a slight decrease in brightness with time and small changes in amplitude from cycle to cycle. Since Ap stars have spots that are stable for years, these small changes are likely

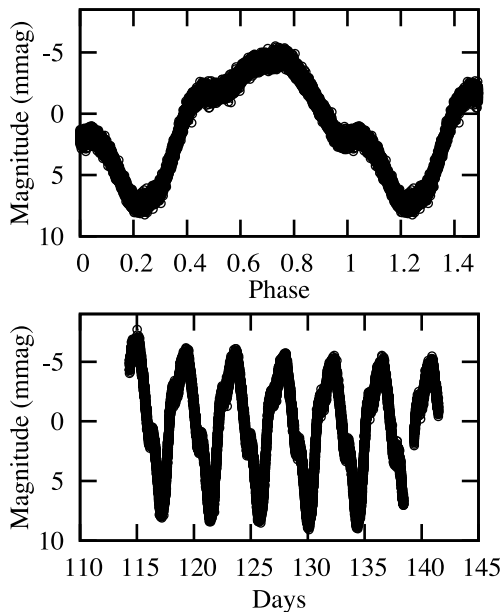


**Figure 2.** Light variation of KIC 10483436. The bottom panel shows the *Kepler* magnitude (in mmag) as a function of time relative to BJD 549 50.000. The top curve shows the data phased with the period  $P_{\text{rot}} = 4.3028$  d.

to be instrumental in origin or a result of the reduction procedure. There is a gap near the end of the run. In order to examine the rotational light curve, we chose not to include the data after the gap, since there is less than one rotational cycle lost. The data before the first minimum in brightness have an anomalously high amplitude which we suspect could be an artefact. We have also excluded these data. The best fit to a ninth-order Fourier fit is obtained with  $P = 4.3022$  d. Some *Kepler* long-cadence data are also available from the commissioning run which can be used to refine the period. This leads to  $P = 4.3028$  d ( $0.2324$  d $^{-1}$ ,  $2.6898$   $\mu$ Hz) with an estimated error of about 0.002 d. The phase diagram using this period and time of phase zero set to BJD 549 50.00 is shown in Fig. 2. The high precision of *Kepler* data gives the impression of high-amplitude rotational modulation, though the peak-to-peak amplitude is only 12 mmag.

It is interesting to examine the frequency components in the low-frequency range. In line with other Ap stars, one expects that there are numerous patches comprising different element abundances and with different surface brightnesses. These patches of different surface brightnesses can be described by a series of spherical harmonics. The smaller the spatial scale, the higher the values of  $l$  and  $m$  required to describe the surface brightness distribution. It is expected that the  $\mu$ mag precision that can be obtained with *Kepler* should enable high values of  $(l, m)$  to be observed, in spite of cancellation effects. By investigating the periodogram at low frequencies one might also hope to estimate the typical size of the patches. However, the inherent ambiguity of the problem prevents us from deducing their exact shape and distribution from the Fourier components. It is possible to study several plausible solutions using simple spot models, but this is usually done in the time-domain. Such an analysis of the KIC 10483436 data is in preparation (Gruberbauer et al., in preparation).

Fig. 3 shows the periodogram of the original data after removing the dominant rotational frequency  $\nu_{\text{rot}} = 0.2324$  d $^{-1}$ . Harmonics as high as  $26\nu_{\text{rot}}$  can be seen and listed in Table 1. Fig. 4 shows the periodogram of the data after removal of a 26th-order Fourier fit to the rotational period. There is no sign of any further rotational harmonics, but there is a low-frequency component of  $0.105$  d $^{-1}$

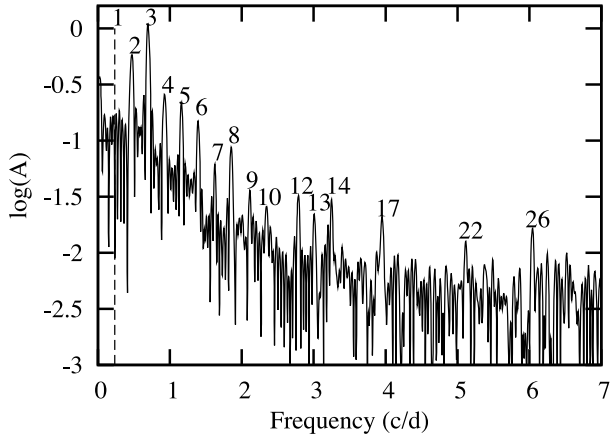


**Figure 3.** The periodogram of KIC 10483436 in the low-frequency region after pre-whitening by the rotational frequency  $\nu_{\text{rot}} = 0.23243 \text{ d}^{-1}$ . The log of the amplitude (in mmag) is plotted against frequency (in cycles  $\text{d}^{-1}$ ). The harmonics of  $\nu_{\text{rot}}$  are indicated.

**Table 1.** Amplitudes ( $A$ , in mmag) and phases ( $\phi$ , in rad) of the rotational frequency,  $\nu_{\text{rot}} = 0.2324 \text{ d}^{-1}$  and its harmonics when the magnitude variation is given by  $A \sin(2\pi n_{\text{H}} \nu_{\text{rot}} t + \phi)$  with the time origin BJD 549 50.0.

$n_{\text{H}}$	$A$ (mmag)	$\phi$ (radians)
1	$5.103 \pm 0.002$	$1.9313 \pm 0.0004$
2	$0.750 \pm 0.002$	$0.1648 \pm 0.0031$
3	$1.283 \pm 0.002$	$-1.6518 \pm 0.0018$
4	$0.331 \pm 0.002$	$-2.9899 \pm 0.0070$
5	$0.205 \pm 0.002$	$-1.3329 \pm 0.0112$
6	$0.148 \pm 0.002$	$-3.1131 \pm 0.0155$
7	$0.046 \pm 0.002$	$-2.8071 \pm 0.0496$
8	$0.095 \pm 0.002$	$-0.7897 \pm 0.0241$
9	$0.034 \pm 0.002$	$-1.1296 \pm 0.0675$
10	$0.036 \pm 0.002$	$-2.9650 \pm 0.0644$
11	$0.004 \pm 0.002$	$2.1330 \pm 0.6492$
12	$0.029 \pm 0.002$	$-1.3649 \pm 0.0781$
13	$0.023 \pm 0.002$	$-0.9178 \pm 0.1006$
14	$0.023 \pm 0.002$	$2.4694 \pm 0.0995$
15	$0.007 \pm 0.002$	$-0.5601 \pm 0.3440$
16	$0.006 \pm 0.002$	$1.9977 \pm 0.3781$
17	$0.023 \pm 0.002$	$1.0569 \pm 0.1016$
18	$0.010 \pm 0.002$	$0.1517 \pm 0.2205$
19	$0.010 \pm 0.002$	$-1.2921 \pm 0.2323$
20	$0.009 \pm 0.002$	$-1.9585 \pm 0.2439$
21	$0.003 \pm 0.002$	$1.3565 \pm 0.8131$
22	$0.014 \pm 0.002$	$-0.6342 \pm 0.1698$
23	$0.003 \pm 0.002$	$-2.2252 \pm 0.8359$
24	$0.004 \pm 0.002$	$0.1216 \pm 0.6377$
25	$0.002 \pm 0.002$	$-1.1565 \pm 1.1233$
26	$0.020 \pm 0.002$	$0.1118 \pm 0.1163$

with amplitude  $80 \mu\text{mag}$  which is most likely an artefact. The highest noise peaks have amplitudes of about  $9 \mu\text{mag}$ . Apart from this, the dominant signal is from the roAp pulsation which will be described below.

#### 4 THE PULSATION FREQUENCIES

Fig. 4 shows a strong signal at about  $1353 \mu\text{Hz}$ . This region is shown in more detail in the bottom panel of Fig. 5, where it is resolved as

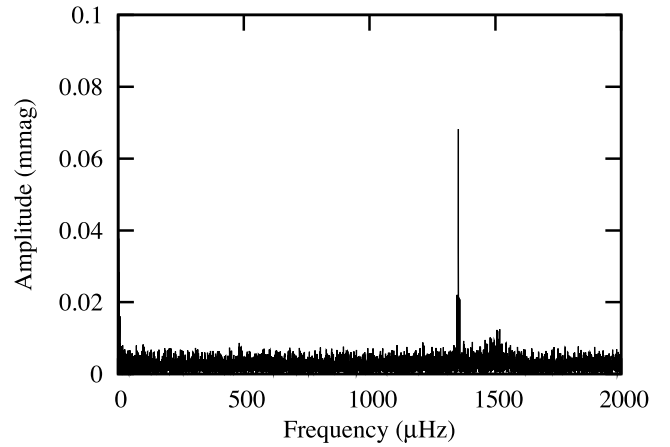


**Figure 4.** The periodogram of KIC 10483436 after removing the rotational variation. The amplitude is in mmag and the frequency in  $\mu\text{Hz}$ .

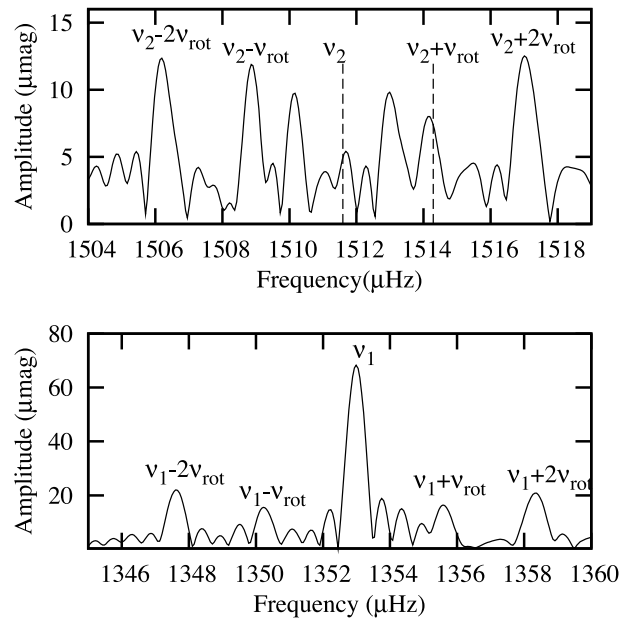


**Figure 5.** Periodograms of KIC 10483436 in two frequency regions. The frequency is in  $\mu\text{Hz}$  and the amplitude in  $\mu\text{mag}$ . Frequencies are labelled as in Table 2. Two apparently missing peaks are shown as dotted lines in the upper panel.

a quintuplet centred on  $\nu_1 = 1353.00 \mu\text{Hz}$  with spacings equal to the rotational frequency  $\nu_{\text{rot}} = 2.6898 \mu\text{Hz}$ . Signals of much lower amplitude at about  $1510 \mu\text{Hz}$  are also visible in Fig. 4 and are shown in more detail in the top panel of Fig. 5. The highest peaks in this region have amplitudes of only about  $12 \mu\text{mag}$  which is not much higher than the highest noise peaks in the periodogram. The three peaks which appear to be significant can be interpreted as part of a quintuplet centred on  $\nu_2 = 1511.62 \mu\text{Hz}$ , though  $\nu_2$  itself is not seen and neither is  $\nu_2 + \nu_{\text{rot}}$ . The false-alarm probability indicates that the other three components are probably real. Table 2 shows the amplitudes and phases calculated on the assumption that the separation of the frequency multiplets is exactly  $\nu_{\text{rot}}$ .

In the simplest form of the oblique pulsator model (Kurtz 1982), a frequency quintuplet, such as that centred on  $\nu_1$  and seen in the bottom panel of Fig. 5, may be interpreted as arising from an obliquely pulsating quadrupole mode. The central peak is the

**Table 2.** Frequencies,  $\nu$ , amplitudes,  $A$ , and phases extracted from *Kepler* data of KIC 10483436 for a magnitude  $\Delta m = \Delta m_0 + \sum_n A_n \sin(2\pi\nu_n t + \phi_n)$ , where the epoch of phase zero is BJD 245 4950.000. In this solution, the rotational multiplets were adjusted in frequency so that their separations are exactly the rotational frequency  $\nu_{\text{rot}} = 2.6898 \mu\text{Hz}$ . FAP is Scargle’s false alarm probability.

	$\nu$ ( $\mu\text{Hz}$ )	$A$ ( $\mu\text{mag}$ )	$\phi$ (rad)	FAP
$\nu_1 - 2\nu_{\text{rot}}$	$1347.62 \pm 0.03$	$21 \pm 2.2$	$-0.20 \pm 0.10$	0
$\nu_1 - \nu_{\text{rot}}$	$1350.31 \pm 0.04$	$15 \pm 2.2$	$0.81 \pm 0.14$	0
$\nu_1$	$1353.00 \pm 0.01$	$69 \pm 2.2$	$-1.71 \pm 0.03$	0
$\nu_1 + \nu_{\text{rot}}$	$1355.69 \pm 0.04$	$15 \pm 2.2$	$0.11 \pm 0.15$	0
$\nu_1 + 2\nu_{\text{rot}}$	$1358.38 \pm 0.03$	$21 \pm 2.2$	$-2.86 \pm 0.10$	0
$\nu_2 - 2\nu_{\text{rot}}$	$1506.23 \pm 0.06$	$12 \pm 2.2$	$2.51 \pm 0.18$	0
$\nu_2 - \nu_{\text{rot}}$	$1508.93 \pm 0.06$	$12 \pm 2.2$	$1.93 \pm 0.18$	0.000 39
$\nu_2$	(1511.62)	$5 \pm 2.2$	$1.59 \pm 0.44$	–
$\nu_2 + \nu_{\text{rot}}$	(1514.30)	$7 \pm 2.2$	$2.08 \pm 0.31$	–
$\nu_2 + 2\nu_{\text{rot}}$	$1516.99 \pm 0.06$	$12 \pm 2.2$	$-2.80 \pm 0.18$	0.000 07

actual pulsation frequency; the rotational sidelobes describe the amplitude and phase modulation of the observed pulsation as it is seen with varying aspect over the rotation cycle. It should be noted, however, that the eigenfunction of an roAp pulsation is far from a simple single spherical harmonic, but is a superposition of spherical harmonics of various degrees.

For  $\nu_1$  one could assume that the dominant spherical harmonic component of the eigenfunction is  $l = 2, m = 0$ . With this assumption, and neglecting other components, the relative amplitudes of the sidelobes give a constraint on the geometry of the pulsation:

$$\tan i \tan \beta = 4 \times \frac{A_{+2}^{(2)} + A_{-2}^{(2)}}{A_{+1}^{(2)} + A_{-1}^{(2)}}$$

where  $i$  is the rotational inclination of the star to the line of sight,  $\beta$  is the obliquity of the pulsation axis to the rotation axis and the amplitudes are for a quadrupole mode [indicated by the superscript (2)] with the identity of the rotational sidelobe given by the subscript (see e.g. Kurtz, Shibahashi & Goode 1990).

Using the amplitudes give in Table 2 for the 1353- $\mu\text{Hz}$  quintuplet, we find

$$\tan i \tan \beta = 4 \times \frac{21.1 \pm 2.2 + 21.1 \pm 2.2}{14.7 \pm 2.2 + 15.1 \pm 2.2} = 5.7 \pm 1.0.$$

This gives the relationship between  $i$  and  $\beta$ , but does not allow us to determine them independently. For that we need a measure of  $\nu \sin i$  from spectroscopy (which we do not yet have), coupled with an estimate of the radius of the star (which is uncertain).

The nature of the multiplets centred on  $\nu_2$  is uncertain because of their very low amplitudes. It would appear that this, too, is a quintuplet, but with the central component and a neighbouring multiplet missing or below the detection level. Considering that even the components that appear to be detected are barely above the noise level, it may be the case that the relative amplitudes shown in Table 2 are greatly distorted. If  $l = 2$  is the dominant spherical harmonic component in both  $\nu_1$  and  $\nu_2$ , as suggested by the fact that they are both quintuplets, then we would expect them to show the same amplitude ratios. Formally, we find for the 1511- $\mu\text{Hz}$  quintuplet  $\tan i \tan \beta = 13.6 \pm 2.9$ , which differs from that for the 1353- $\mu\text{Hz}$  quintuplet by  $2.4\sigma$ , which is not statistically significant.

A more interesting test is to look at the amplitude of the missing central peak for the 1511- $\mu\text{Hz}$  quintuplet. If the amplitude ratio

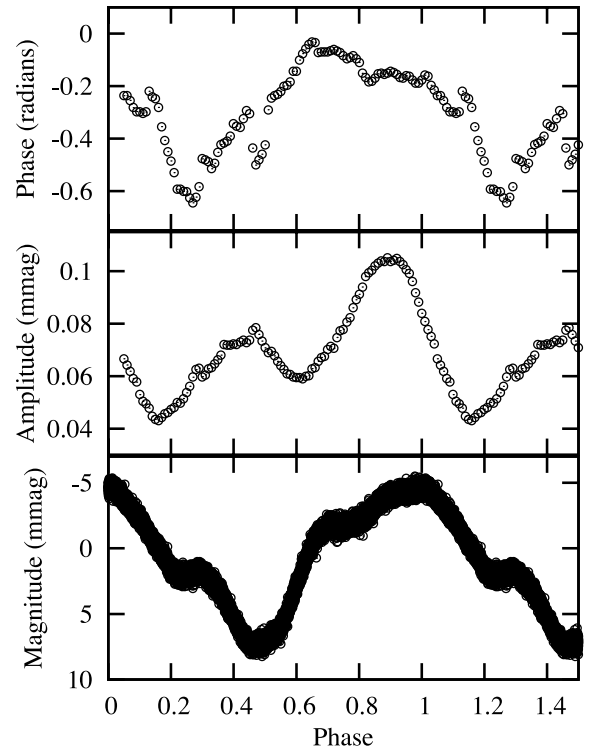


**Figure 6.** Bottom panel: light curve (in mmag) of KIC 10483436 phased with  $P = 4.3038$  d and time of phase zero (light maximum) BJD 549 53.2363. Middle panel: the amplitude of the 1353- $\mu\text{Hz}$  pulsation mode (in mmag). Top panel: the phase of the 1353- $\mu\text{Hz}$  pulsation mode (in rad).

$\frac{A_{+2}^{(2)} + A_{-2}^{(2)}}{A_0^{(2)}}$  is the same for both quintuplets – as it should be if they arise from the same degree mode, have the same pulsation axis and are perturbed similarly by the magnetic field – then we can predict from that ratio for the 1353- $\mu\text{Hz}$  mode,  $0.62 \pm 0.04$ , that the central peak of the 1511- $\mu\text{Hz}$  mode should have an amplitude of  $44 \mu\text{mag}$ . This is clearly ruled out in the top panel of Fig. 5. Unfortunately, the amplitudes of these multiplets are very close to the noise level. This means that we cannot fully identify the rotational sidelobes (if they exist). Any deductions that could be made from the 1511- $\mu\text{Hz}$  mode must await further data which, hopefully, will increase the signal-to-noise ratio.

One can measure the amplitude and phase as a function of time by using a sliding window and fitting a sinusoid to data in this window. Fig. 6 shows how the amplitude and phase of  $\nu_1$  vary with rotational phase using a sliding window of 33 min total width and finding the mean in 100 phase bins. The figure shows two maxima per rotation cycle, consistent with a predominantly quadrupole mode. The maximum pulsational amplitude occurs at the rotational phase  $\phi = 0.90$  (maximum light occurs at  $\phi = 0.0$ ). The secondary maximum is at phase  $\phi = 0.46$ , rather close to minimum light at  $\phi = 0.47$ .

In roAp stars, the maximum pulsation amplitude occurs when the magnetic pole is closest to the line of sight. That this is not the time of rotational maximum brightness probably indicates that the complex spots are not coincident with the magnetic/pulsation pole. This was clearly shown to be the case for the roAp star  $\alpha$  Cir (Bruntt et al. 2009), where the rotational variation, as measured from space with the *WIRE* mission, has an amplitude of only a few mmag. We expect more Ap stars to be found with spots that are not symmetric about the magnetic axis as higher precision

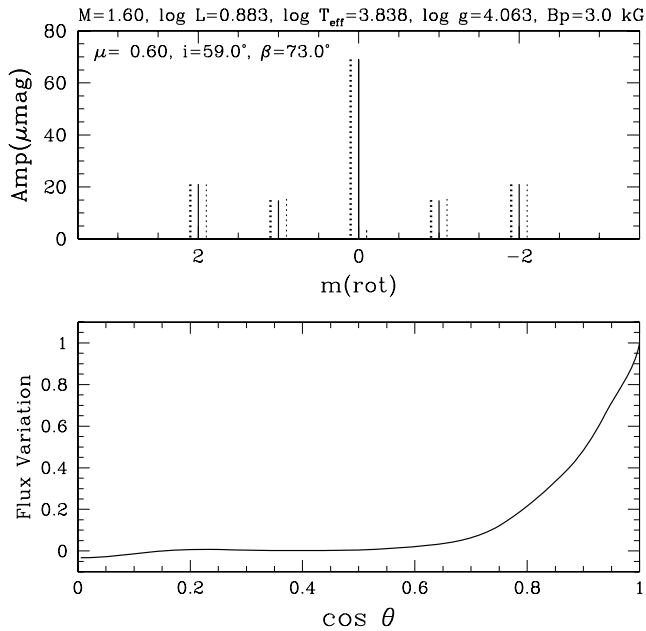


**Figure 7.** Bottom panel: variation in the surface eigenfunction with colatitude,  $\theta$ , measured from the magnetic axis. The eigenfunction for this axisymmetric quadrupole mode was calculated for a  $1.6\text{-}M_{\odot}$  model and a polar field strength of  $B_p = 3\text{ kG}$ . Top panel: the solid lines are relative amplitudes for the  $1353\text{-}\mu\text{Hz}$  multiplet as calculated using the eigenfunction shown in the bottom panel. We assume  $(i, \beta) = (59^\circ, 73^\circ)$ . The observed amplitudes are indicated by the thick solid lines which are shifted slightly to the left-hand side for clarity. The thin dotted lines shifted slightly to the right-hand side are relative amplitudes calculated using a spherical harmonic  $Y_{l=2}^{m=0}(\theta, \phi)$ . The amplitude is normalized to the observed amplitude for  $\nu_1 - 2\nu_{\text{rot}}$ .

observations become available for these stars. The phase variation of the  $1353\text{-}\mu\text{Hz}$  mode (Fig. 6) is not well defined, but does appear to vary by about  $0.5$  rad.

## 5 MAGNETIC EFFECTS

In the previous section,  $\tan i \tan \beta$  was estimated assuming the eigenfunction for the frequency  $\nu_1$  to be proportional to a spherical harmonic of  $(l, m) = (2, 0)$ . In reality, the eigenfunction is far from a simple spherical harmonic and is modified by the magnetic field which is typically a few kG in roAp stars. Hence, the relative amplitudes in a multiplet will also be modified. For a dipolar magnetic field, the deformation from the spherical harmonic  $Y_{l=2}^{m=0}(\theta, \phi)$  can be represented by taking into account contributions from the  $l = 0, 4, 6, \dots$  components.

The bottom panel of Fig. 7 shows the latitudinal amplitude variation of a quadrupole mode in a  $1.6\text{-}M_{\odot}$  model with a dipolar magnetic field and with the polar field strength  $B_p = 3\text{ kG}$  and pulsation frequency of  $1352\text{ }\mu\text{Hz}$ . This was obtained by a non-adiabatic analysis using the method discussed in Saio (2005). Obviously, the amplitude variation deviates significantly from the Legendre function  $P_2(\cos \theta)$ , being strongly confined to the polar region due to the considerable effects of the  $l = 0$  and  $4$  components. The relative amplitudes of a multiplet can be obtained by integrating the eigenfunction over the stellar disc, assuming the brightness is proportional to  $(1 - \mu + \mu \cos \Theta)$ , where  $\mu$  is the limb-darkening parameter (a standard value of  $0.6$  is adopted here) and  $\Theta$  is the colatitude with respect to the line of sight (see Saio & Gautschi 2004, for details).

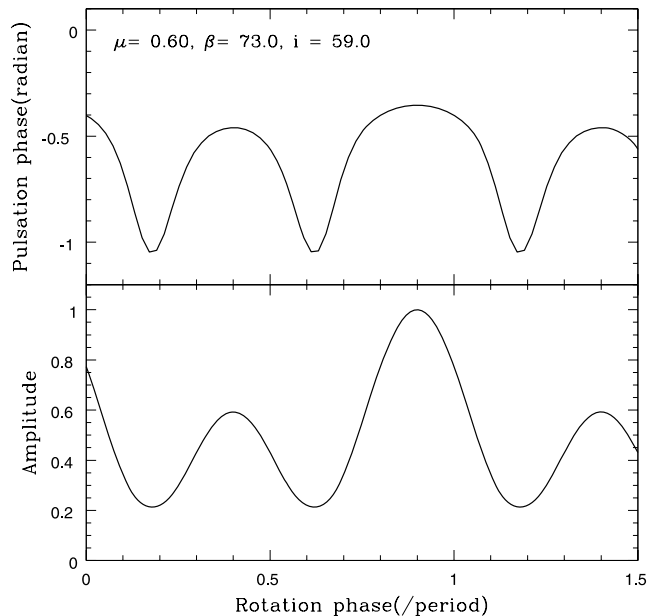


**Figure 8.** Theoretical amplitude (bottom panel) and phase (top panel) variation for the  $1353\text{-}\mu\text{Hz}$  mode as a function of rotational phase. Phase zero is chosen so that the maximum amplitude occurs at phase  $0.9$  as in Fig. 6. The top panel shows the phase of the radial component of the mode measured from the instance when the luminosity variation is zero at the negative to positive crossing.

Using this eigenfunction, we searched for a set of angles  $(i, \beta)$  which best reproduce the relative amplitudes of the  $1353\text{-}\mu\text{Hz}$  quintuplet. The best case, which is obtained with  $(i, \beta) = (59^\circ, 73^\circ)$ , is shown by the solid lines in the top panel of Fig. 7. These are to be compared with the observed amplitudes shown by the thick dotted lines slightly shifted to the left-hand side. We note that the result is independent of interchanging  $i$  and  $\beta$ . In addition, since the theoretical results change only slowly with  $i$  and  $\beta$ , the good agreement is retained even when these angles are changed by as much as  $\pm 5^\circ$ . It is interesting to note that the best value for the rotational inclination angle is compatible with those obtained from spot models for the rotational modulation to the light curve of KIC 10483436 (Gruberbauer et al., in preparation).

For  $(i, \beta) = (59^\circ, 73^\circ)$ ,  $\tan i \tan \beta = 5.44$  is consistent with the value estimated in the previous section from the amplitude ratio between  $A_{\pm 1}$  and  $A_{\pm 2}$ , assuming the pure harmonic function  $Y_{l=2}^{m=0}$ . We note, however, that an  $l = 0$  component is definitely needed to be consistent with the observed amplitude of the central component of the quintuplet. This amplitude is very small if a pure  $Y_{l=2}^{m=0}$  is used, as shown in the top panel of Fig. 7 by the thin dotted lines shifted slightly to the right-hand side. In other words, the observed relative amplitudes in the  $1353\text{-}\mu\text{Hz}$  quintuplet indicate clearly the presence of a considerable magnetic effect on the eigenfunction.

Fig. 8 shows the theoretical luminosity amplitude (bottom panel) and phase (top panel) variation as a function of rotational phase. In the figure, the rotational phase is adjusted so that the maximum luminosity amplitude occurs at a rotational phase of  $0.9$  as in Fig. 6. The calculated amplitude variation agrees quite well with the observations, which is not surprising because it contains the same information as the amplitude spectrum of the quintuplet shown in Fig. 7. However, the calculated phase variation is considerably different from the observations, though the phase range, about  $0.5$  rad, is in agreement. The cause of the discrepancy is not clear. The

inhomogeneous surface brightness distribution due to abundance patches is not included in the present model and may possibly affect the phase variation.

The model used in the above discussion has  $(M, \log T_{\text{eff}}, B_p) = (1.6 M_{\odot}, 3.838, 3 \text{ kG})$ . This model identifies the frequencies  $\nu_1$  and  $\nu_2$  as a quadrupole mode (1352  $\mu\text{Hz}$ ) with radial order 21 and a dipole mode (1514  $\mu\text{Hz}$ ) with radial order 24, respectively. These theoretical frequencies agree quite well with the observed frequencies, although the effective temperature of the model is somewhat lower than the value from the KIC (Section 2). The magnetic field strength was chosen such that the eigenfunction of the quadrupole mode has a sufficient contribution from the  $l = 0$  and 4 components to be consistent with the relative amplitudes of the  $\nu_1$  quintuplet. To obtain agreement of the relative amplitudes, our model requires a magnetic field of about  $B_p \approx 3 \text{ kG}$ . If observations can confirm a polar magnetic field of about this strength, it would lend confidence to the theory given in Saio (2005) and Saio & Gautschy (2004).

In this model, several modes are excited due to the  $\kappa$  mechanism in the hydrogen ionization zone (Cunha 2002). The 1352- $\mu\text{Hz}$  quadrupole mode is excited, while the 1514- $\mu\text{Hz}$  dipole mode is marginally damped. This might explain why the amplitude of  $\nu_1$  is so much larger than the amplitude of  $\nu_2$ . However, we cannot explain why several other modes which are unstable in the model are not observed. Spectroscopic observations will be required to better constrain the models.

## 6 DISCUSSION

An interesting aspect of KIC 10483436 is that rotational modulation with a modest peak-to-peak amplitude of only 12 mmag was observed with such clarity that we were able to detect harmonics of the rotation frequency up to  $26\nu_{\text{rot}}$ . This indicates significant small-scale structure to the abundance spots on the star. From the rotational variation, we derived a rotational period of  $4.3028 \pm 0.002 \text{ d}$ . With such a short rotation period, the expected multiplets from the oblique pulsator model were observed in one mode at 1353  $\mu\text{Hz}$ . We were also able to detect another mode at around 1510  $\mu\text{Hz}$ , but with amplitudes too close to the detection limit to be useful. Further observations of this star may lead to an increase in the signal-to-noise ratio, which may then allow a proper analysis of this mode.

With a 4-d rotation period and  $R = 1.6 R_{\odot}$ , we expect an equatorial rotation velocity for KIC 10483436 of  $v_{\text{rot}} \approx 20 \text{ km s}^{-1}$ . If  $i \approx 60^\circ - 70^\circ$ , then it may be possible to study the surface spots with spectroscopic Doppler Imaging.

The two pulsation modes detected have frequencies separated by 158  $\mu\text{Hz}$ . The models predict unstable modes with frequencies between the two observed modes, but these are not observed. This is the case for another roAp star, HD 217522 (Kreidl et al. 1991), so it is not without precedent, but why these modes are not observed is not presently understood. In KIC 8677585, a mode at low frequency typical of  $\gamma$  Dor stars was observed. No such low-frequency modes were detected in KIC 10483436.

As with KIC 8677585, the amplitudes of the modes exhibited by KIC 10483436 are only a few tens of  $\mu\text{mag}$ . These could not

have been observed if it were not for the extremely low noise level attained with *Kepler* data. Had these two stars been observed photometrically from ground, they would have been classified as noAp stars. Therefore, the results presented here and in the paper by Balona et al. (2011) emphasize the need to consider the possibility that stars classified as noAp may well be low-amplitude roAp stars. In that case, any systematic differences found between the two groups – roAp and noAp stars – should be thought in terms of the physical aspects that determine the amplitude of the pulsations, rather than in terms of the driving mechanism.

## ACKNOWLEDGMENTS

The authors wish to thank the *Kepler* team for their generosity in allowing the data to be released to the Kepler Asteroseismic Science Consortium (KASC) ahead of public release and for their outstanding efforts which have made these results possible. Funding for the *Kepler* mission is provided by NASA's Science Mission Directorate. We particularly thank Ron Gilliland for his tireless work on behalf of the KASC.

LAB wishes to thank the South African Astronomical Observatory for financial support.

This work was partially supported by the project PTDC/CTE-AST/098754/2008 funded by FCT/MCTES, Portugal. MSC is supported by a Ciência 2007 contract, funded by FCT/MCTES (Portugal) and POPH/FSE (EC).

MG has received financial support through D. Guenther's NSERC grant.

## REFERENCES

- Balmforth N. J., Cunha M. S., Dolez N., Gough D. O., Vauclair S., 2001, *MNRAS*, 323, 362
- Balona L. et al., 2011, *MNRAS*, 410, 517
- Bigot L., Dziembowski W. A., 2002, *A&A*, 391, 235
- Borucki W. J. et al., 2010, *Sci*, 327, 977
- Bruntt H. et al., 2009, *MNRAS*, 396, 1189
- Cunha M. S., 2002, *MNRAS*, 333, 47
- Cunha M. S., Gough D., 2000, *MNRAS*, 319, 1020
- Dziembowski W. A., Goode P. R., 1996, *ApJ*, 458, 338
- Gilliland R. L. et al., 2010, *ApJ*, 713, L160
- Gough D., 2005, in Bowler S., ed., *The Roger Tayler Memorial Lectures 1999–2003. Astron. Geophys., Special Issue*, p. 16
- Jenkins J. M. et al., 2010, *ApJ*, 713, L87
- Koch D. G. et al., 2010, *ApJ*, 713, L79
- Kreidl T. J., Kurtz D. W., Bus S. J., Kuschnig R., Birch P. B., Candy M. P., Weiss W. W., 1991, *MNRAS*, 250, 477
- Kurtz D. W., 1982, *MNRAS*, 200, 807
- Kurtz D. W., Shibahashi H., Goode P. R., 1990, *MNRAS*, 247, 558
- North P., Jaschek C., Hauck B., Figueras F., Torra J., Kunzli M., 1997, in Battrick B., ed., *Proc. ESA Symp. 402, Absolute Magnitudes of Chemically Peculiar Stars*. ESA, Noordwijk, p. 239
- Saio H., 2005, *MNRAS*, 360, 1022
- Saio H., Gautschy A., 2004, *MNRAS*, 350, 485
- Théado S., Dupret M., Noels A., Ferguson J. W., 2009, *A&A*, 493, 159

This paper has been typeset from a  $\text{\TeX}/\text{\LaTeX}$  file prepared by the author.